Sodium bicarbonate nanoparticles modulate the tumor pH and enhance the cellular uptake of doxorubicin

Hanan Abumanhal-Masarweh[1,2], Lilach Koren[1], Assaf Zinger[1], Zvi Yaari[1], Nitzan Krinsky[1,3], Galoz Kaneti[1], Nitsan Dahan[4], Yael Lupu-Haber[4], Edith Suss-Toby[5], Esther Weiss-Messer[5], Michal Schlesinger-Laufer[6], Janna Shainsky-Roitman[1] and Avi Schroeder[1,*]

[1]Laboratory for Targeted Drug Delivery and Personalized Medicine Technologies, Department of Chemical Engineering, Technion – Israel Institute of Technology, Haifa 32000, Israel
[2]Russell Berrie Nanotechnology Institute, The Norman Seiden Multidisciplinary Graduate program, Technion – Israel Institute of Technology, Haifa 3200, Israel
[3]The Interdisciplinary Program for Biotechnology, Technion – Israel Institute of Technology, Haifa 32000, Israel
[4]Life Sciences and Engineering Infrastructure Center, Lorry I. Lokey Interdisciplinary Center, Technion – Israel Institute of Technology, Haifa 32000, Israel
[5]Bioimging Center, Biomedical Core Facility, Ruth and Bruce Rappaport Faculty of Medicine, Technion – Israel Institute of Technology, Haifa 32000, Israel
[6]The Pre-Clinical Research Authority Unit, Technion – Israel Institute of Technology, Haifa 32000, Israel

[*]E-mail: avids@technion.ac.il

Abstract

Acidic pH in the tumor microenvironment is associated with cancer metabolism and creates a physiological barrier that prevents from drugs to penetrate cells. Specifically, ionizable weak-base drugs, such as doxorubicin, freely permeate membranes in their uncharged form, however, in the acidic tumor microenvironment these drugs become charged and their cellular permeability is retarded. In this study, 100-nm liposomes loaded with sodium bicarbonate were used as adjuvants to elevate the tumor pH. Combined treatment of triple-negative breast cancer cells (4T1) with doxorubicin and sodium-bicarbonate enhanced drug uptake and increased its anti-cancer activity. *In vivo*, mice bearing orthotropic 4T1 breast cancer tumors were administered either liposomal or free bicarbonate intravenously. 3.7±0.3% of the injected liposomal dose was detected in the tumor after twenty-four hours, compared to 0.17%±0.04% in the group injected free non-liposomal bicarbonate, a 21-fold increase. Analyzing nanoparticle biodistribution within the tumor tissue revealed that 93% of the PEGylated liposomes accumulated in the extracellular matrix, while 7% were detected intracellularly. Mice administered bicarbonate-loaded liposomes reached an intra-tumor pH value of 7.38±0.04. Treating tumors with liposomal bicarbonate combined with a sub-therapeutic dose of doxorubicin achieved an improved therapeutic outcome, compared to mice treated with doxorubicin or bicarbonate alone. Interestingly, analysis of the tumor microenvironment demonstrated an increase in immune cell' population (T-cell, B-cell and macrophages) in tumors treated with liposomal bicarbonate. This study demonstrates that targeting metabolic adjuvants with nanoparticles to the tumor microenvironment can enhance anticancer drug activity and improve treatment.

Keywords: nanoparticle, breast cancer, pH, immune system, microenvironment, metabolism, bicarbonate

Introduction

In 1924, Otto Heinrich Warburg demonstrated that cancer cells overproduce lactate by anaerobic glycolysis, even in the presence of a sufficient oxygen supply [1-3]. Combined with the increased glucose metabolism in tumors, high lactate production corresponds to high proton concentrations. Accompanied with poor perfusion, this results in an acidic extracellular pH ranging from 6.5 to 6.9 in malignant tumors, compared to the normal 7.4 physiological pH [1, 3, 4]. These acidic conditions are associated with cancer cell survival, migration, metastasis and increased expression of the multidrug drug resistance efflux transporter p-glycoprotein (pGP) [1, 3, 5]. Several studies have considered the acidic pH within the tumor microenvironment as a potential therapeutic target [6, 7].

Tumor chemosensitivity is also affected by the extracellular acidic pH which forms a physiological drug barrier, a phenomenon known as 'ion trapping'. For example, ionizable weak-base drugs such as doxorubicin, mitoxantrone and daunorubicin freely permeate membranes in their uncharged form [6, 7]. Doxorubicin for example, is a DNA-intercalating chemotherapeutic commonly used for treating primary and metastatic breast cancer; however, chemically being a weak-base doxorubicin undergoes ‘ion trapping’ in the acidic tumor environment, reducing its cellular uptake and efficacy [8-10]. In acidic environments, weak bases become charged and their permeability through the lipid-based cell membrane is inhibited [5, 7].

Bicarbonate is a natural alkaline buffer that regulates blood and tissue pH [11, 12]. Through the secretion of $CO_{2(g)}$, ($CO_{2(g)} + H_2O \rightleftharpoons H_2CO_3 \rightleftharpoons HCO_3^- + H^+$) bicarbonate creates a continuously increasing alkaline pH in solution. At 37°C the rate of conversion of CO_2 to bicarbonate (H_2CO_3) is $k = 5.4\times10^{-5}$, reaching an equilibrium ratio of 340:1, $[CO_2]$:$[H_2CO_3]$ respectively [13]. Carbonic anhydrase counters this reaction, converting CO_2 equilibrium towards the right-hand of the equation and acidifying the tumor microenvironment [13]. As such, this enzyme has become a therapeutic target, found to be associated with tumor malignancy, metastases and poor response to chemotherapy [7, 14, 15]**.**

Bicarbonate is a potential candidate molecule for increasing the activity, bioavailability and potency of chemotherapeutic agents that are retarded in the acidic tumor microenvironment [9, 11]. Previous studies [4, 11], have suggested consuming sodium

bicarbonate orally as a mean for elevating the tumor pH and improving therapeutic activity. However, poor biodistribution and dilution of the bicarbonate after being absorbed through the gastrointestinal tract resulted in insufficient bicarbonate delivery to the tumor. Herein, we suggested that a nanoparticulate form of sodium bicarbonate may improve the tumor targeting capacity.

Nanotechnologies are becoming important medical tools, owned to their ability to target therapeutic and diagnostic compounds to diseased tissues with high accuracy [16-27]. Specifically, nanoparticles have been shown to accumulate preferentially in solid tumors by extravagating through defects in the endothelial layer of the tumor vasculature, a phenomenon known as the Enhanced Permeation and Retention (EPR) effect [28-34] Liposomes, self-assembled vesicles, having one or several concentric lipid bilayers, are widely used nanoscale drug delivery systems [35]. One-hundred nanometer PEGylated liposomes loaded with doxorubicin (Doxil) are FDA-approved for treating metastatic breast cancer, and have been shown to accumulate preferentially in tumors due to the EPR effect [36-38]. In addition, cell culture experiments showed that ammonium bicarbonate can increase liposomal doxorubicin release and enhance its activity [37]. Moreover, liposomal ammonium bicarbonate was prepared as a gas-generating nanoparticle used for photoacoustic imaging of murine breast cancer tumors [39]. Som et al. also demonstrated that calcium carbonate nanoparticles increase tumor pH post intravenous administration [40]. In this work, 100-nm PEGylated liposomes were evaluated for their capacity to act as an adjuvant and enhance the anticancer activity of doxorubicin *in vitro* and *in vivo*, by delivering sodium bicarbonate to triple-negative breast cancer tumors. We found that the use of bicarbonate liposomes increased the uptake and therapeutic activity of doxorubicin. These studies highlight the tumor stroma as an important therapeutic target for improving treatment outcome**.**

Materials and methods

Cell culture.

Triple negative breast cancer cell line, 4T1 (ATCC) was grown in RPMI 1640 (Biological Industries, Beit Haemek, Israel) supplemented with 10% v/v of heated inactivated fetal calf serum (Biological Industries, Beit Haemek, Israel), 1% v/v Penicillin-Streptomycin solution (10 000 U/ml of Penicillin G Sodium Salt and 10 mg/ml of Streptomycin Sulfate), and 1% v/v L-Glutamine (Biological Industries, Beit Haemek, Israel). Cells were cultured at 37°C in a humidified atmosphere and 5% CO_2 in air.

Breast cancer animal model.

Eight to ten week-old BALB/c female mice (Harlan laboratories, Jerusalem, Israel) were used as breast cancer animal models; 50 µl of $2.5x10^5$ 4T1 cells in phosphate-buffered saline (PBS) were injected subcutaneously into the mammary fat pad to obtain primary tumor model. Mice weights were recorded every other day; once a tumors' size of 100-200mm^3 on average was observed, the mice were divided to different treatments groups. All animal procedures were performed according to guidelines of the Institutional Animal Research Ethical Committee.

Liposomes formulation.

To obtain liposomes with final lipid concentration of 50mM composed of 55% mol hydrogenated soybean phosphatidylcholine (HSPC, MW 762 gr/mol, Lipoid, Ludwigshafen, Germany), 5% mol polyethyleneglycol distearoyl-phosphoethanolamine (m2000PEG DSPE, Lipoid), and 40% mol cholesterol (MW 386.6, Sigma Aldrich, Rehovot, Israel), accurately weighed amounts of lipids were dissolved in absolute ethanol (BioLab, Jerusalem, Israel), and warmed to 65°C. Once all the lipids were completely dissolved in ethanol, the lipid suspension was added to 65°C warmed 5% (%w/v) dextrose solution (Sigma Aldrich, Rehovot, Israel) containing 0.5M sodium bicarbonate (Frutaruom, Haifa, Israel) to form multi laminar vesicles (MLVs). To obtain homogenous liposomes, the mixture of lipids was passed stepwise extrusion through 400, 200 ,100 and 80nm pore-size polycarbonate membranes (GE Osmonics, USA), in extruder supplied with a warm circulating bath (Northern Lipids, Vancouver, Canada). Then liposomes solution

was dialyzed against 5% dextrose using a 12-14 kDa dialysis membrane. The dextrose solution was replaced after 1, 4 and 24 hours, to ensure removal of all non-entrapped molecules.

Doxorubicin liposomes were prepared by an active loading method; ammonium sulfate gradient, was used to load doxorubicin according to Haran et al. [41]. The non-encapsulated drugs were removed by dialysis, as described previously. Liposomes size analysis, which includes mean diameter (nm) and particle size distribution (PDI) measurements, were carried out by dynamic light scattering (DLS) with a backward angle of 173° using a Zetasizer Nano ZSP (Malvern, UK). Measurements were made at room temperature.

pH measurements of the liposomal aqueous phase.

pH Measurements of the liposomal bicarbonate internal aqueous phase were obtained using pyranine, a fluorescent pH indicator. Determination of pH by pyranine is based on the ratio of fluorescence intensity at an emission wavelength of 510 nm measured at two excitation wavelengths: at 460 nm-which is pH dependent, and at 415 nm, the pH-independent isosbestic point. The liposomes internal phase pH values were calculated as described by Avnir et al. [42]. A calibration curve was plotted using solver XLaM, and the pH values were calculated from the 460/415-nm excitation ratio of the fluorescence intensities.

Moreover, direct pH measurements of the aqueous phase were measured using pH meter after applying Bligh and Dyer assay on the liposomes [43]. Briefly, according to the sample volume, a mixture of 1:2 chloroform:methanol, was added to the liposomes then chloroform was added followed by addition of DDW, each step was followed by vortex. The sample was then centrifuged at 1000 RPM for 5min and a two phase system was created (aqueous and lipid phases). After getting two separated phases, pH meter (cybersacn pH 11, Thermo Scientific) was used to measure the pH in the obtained aqueous phase. Since Bligh and Dyer upper phase is composed of water, methanol and some chloroform which could affect the pH, a calibration curve that compares the pH in aqueous phase as is and after it is extracted was conducted and results were normalized according to that. Three solutions with different pH values (4, 7 and 10) were processed using the

Bligh and Dyer method. Then, for each solution, the pH of the aqueous phase was measured and the effect of the methanol presence was found to induce a maximal shift of 1.03±0.27 pH units. This value was subtracted from our measurements to obtain the corrected value.

Sodium bicarbonate liposomal content.

Sodium bicarbonate liposomal content was quantified using Inductively Coupled Plasma (ICP-OES 5100, Agilent Technologies, Santa Clara, CA, USA). Empty liposomes were used as a negative control. Na concentration of each sample was measured using a standard calibration curve between 0.01 and 50 ppm (dissolved in 1% nitric acid). Encapsulation efficiency of sodium bicarbonate liposomes was calculated as the ratio of Na quantified in liposomes to 5% w/v dextrose solution containing 0.5M sodium bicarbonate.

Cells viability and chemosensitivity assays.

4T1 cells were seeded onto 96-wells plate at $2.5x10^4$ cells in 200µl medium per well and allowed to attach overnight. Chemosensitivity of the cultured cells was examined by incubating the cells with 0.5µg/ml doxorubicin in cell culture media with different pH. Cell culture media with various pH values was prepared by titration of RPMI 1640, with HCl (0.1M). Cell viability was determined using Cell Titer-Glo Luminescent cell viability assay (Promega) 24 hours after treatment's application. Similarly, the cytotoxicity of cisplatin (3.8µg/ml) and 5-fluorouracil (1.3 µg/ml) were evaluated under the same conditions as described above. Cell viability was determined using a commercial MTT viability assay (Sigma Aldrich, Rehovot, Israel).

Evaluation of Doxorubicin cellular uptake by Flow-cytometry.

4T1 cells were seeded onto 6-well plate at density of 10^5 cells per well in 2 ml of RPMI incubated for 24h (37 °C, 5% CO_2). The cells were then incubated with 5µg/ml free doxorubicin with or without sodium bicarbonate (50mM) in cell culture media at different pH points (6.5 and 7.4). After 18 hours the culture media was removed and the cells were rinsed with PBS for three times to remove the drug. The cells were harvested by trypsinization and resuspended in PBS after centrifugation (1000 rpm, 5 min) and Flow

cytometry was done using BD LSR-II Analyzer (Biosciences, San Jose, CA, USA). Results were analyzed using FCS Express (De Novo software).

Confocal laser scanning microscopy (CLSM) observation.

Confocal laser scanning microscopy (CLSM) was employed to examine the intracellular uptake of doxorubicin .4T1 cells were seeded on 8 wells µ-slide (Ibidi) at density of $4X10^4$ cells per well in 700 µl of RPMI incubated for 24 h (37 °C, 5% CO_2), the cells were then incubated with 10µg/ml free doxorubicin with or without sodium bicarbonate (50mM) in RPMI with different pH points (6.5 and 7.4) for 4 h at (37 °C, 5% CO_2). The culture media was removed and the cells were rinsed with PBS for three times to remove the drug. Then the nuclei were stained with Hoechst (1µg/ml) at 37 °C for 15 min. LSM 710 inverted confocal microscope was used to obtain Fluorescence images for doxorubicin cellular uptake. Acquisition was performed using the ZEN software and applying the 405 and 488 lasers.

For statistical analysis, cells were seeded in 24-well plates at a density of $8X10^4$ cells per well, and incubated for 24 h (37 °C and 5% CO_2). Cells were treated at the same conditions described above, and each plate was scanned using a GE InCell Analyzer2000 to obtain random images (12 fields per well, and 4 wells per each treatment group). The obtained images were analyzed using the InCell software to quantify doxorubicin fluorescent intensity in the cytoplasm and nuclei.

Quantification of intra cellular Doxorubicin after enzymatic desequestration.

Cells were grown in 24-well plates at a density of $2X10^5$ cells per well in 700 µl, and incubated for 24 h (37 °C, 5% CO_2). Cells were then incubated with 10µg/ml free doxorubicin, with or without sodium bicarbonate (50mM) in RPMI, at pH 6.5 and 7.4, for 4 h at (37 °C, 5% CO_2). After treatment, cells were washed twice with PBS (500 µl per well) and then harvested with 200 µl trypsin. Cells were centrifuged and suspended in 400 µl PBS. Cells were lysed as described by Anders Andersen et al [44]. Briefly 10µl Triton X-100 (5%) and 10µl proteinase K (10 mg/ml) were added and mixed. Samples were incubated for 1h at 65ºC. Then 5µl phenylmethanesulfonyl fluoride (PMSF, 10 mM in isopropanol) was added. Samples were left at room temperature for 10 min. 10 µl MgCl2

(0.4 M) and 20 µl DNase I (1 mg/ml) were then added and samples were incubated at 37 °C for 30 min. Deproteinization was done by adding 450 µl methanol and 45 µl ZnSO4 (400 mg/ml) to all samples. The samples were then centrifuged at 15,000 X g for 5 min. 100 µl X4 of the supernatant was transferred to 96 flat bottom black polystyrene plate. Doxorubicin calibration curve (0.15µg/ml to 10 µg/ml) was prepared by dissolving the drug in methanol. Doxorubicin fluorescent intensity (excitation 488nm, emission 560nm) was measured using a Tecan (Mannedorf, Switzerland) plate reader.

Quantitative liposomes distribution in the tumor tissue.

Once the tumors evolved (around 500-700mm^3), mice were divided randomly into two groups and were injected intravenously with either 300µl sodium bicarbonate and Gd-loaded liposomes (90 nm, 50mM lipid) or with 300µl of Free Gd sodium bicarbonate solution. Twenty-four hours after the injection, the mice were sacrificed and tumors were extracted. Samples were heated to 500˚C for 5 hours and their ash dissolved in nitric acid 1% (Bio Labs, Israel). Gd concentration of each sample is measured using a standard calibration curve at 0.01, 0.05, 0.1, 0.5, 1.0, 5.0 and 10 ppm. Gd was quantified using Inductively Coupled Plasma – Optical Emission Spectroscopy (ICP-OES, 5100-Agilent).
For tumor cell/ECM (Extra cellular matrix) biodistribution study, Gadolinium-encapsulated liposomes were injected intravenously to BALB/c female mice (n=6). 24 hours later, tumors were extracted and dissociated into a cell suspension or ECM fractions using a gentleMACS Tissue Dissociator (Miltenyi Biotec, Teterow, Germany). To obtain two compartments, ECM and single cell suspension, an enzyme mix for degrading the ECM was prepared as follows: 25mg/ml Hyaluronidase (Sigma Aldrich), 25mg/ml Collagenase-III (Worthington Biochemical, Lakewood, NJ, USA), and 50mg/ml Collagenase-IV (Worthington Biochemical). After 45 min incubation with the tissue, freed cells were centrifuged, the supernatant was kept and lyophilized, the cells sediment was suspended in 500µl PBS. Samples were heated to 500 ˚C for 5 hours and their ash was dissolved in nitric acid 1% (Bio Labs, Israel). Gd concentration of each sample was quantified as described above. The ratio of Gd quantity in the cell' compartment versus the ECM was calculated.

Measurements of *in-vivo* interstitial pH.

pH measurements were applied as described in Veronica Estrella et al. [3].Briefly, 4T1 cells are grown as subcutaneous tumors. Once tumors reach a volume of 500-800 mm^3, the extracellular pH is measured by microelectrode using pH meter (cybersacn pH 11, Thermo Scientific). At first, animals were sedated with isoflurane (2.5-3.5%). Reference and pH electrode (MI-401F and MI-408B, respectively, Microelectrodes) were used to measure the pH levels. Initially, the reference electrode (outer diameter, 1 mm) was inserted under the skin of the mouse near the tumor, then the pH electrode (outer diameter, 0.8 mm) is then inserted up to 1.3 cm into the center of each subcutaneous tumor. Electrodes were calibrated before and following each set of measurements using standard pH 4, 7 and 10 buffers. Three measurements were taken at each position and 3 positions interrogated and averaged per one mouse.

Ultrasound scanning of breast cancer tumors.

Once the tumors evolved (around 500-700mm^3), Mice were anesthetized with 1.5-2% isoflurane and kept at 37 ^oC. Tumors were scanned using Vevo2100 Micro-ultrasound imaging system (Visualsonics) equipped with 21MHz (MS-250) transducer for abdominal imaging. B-Mode and Contrast-Mode recordings were performed on tumors before, throughout (up to 14 secs approx. using pre trigger option) and after (1min after) liposomes IV injection. Mice were scanned up to 5 min after liposomes injection, the increase in contrast mean power measured with bicarbonate liposomes was kept during this period of time. Data was analyzed using VevoLab software.

***In vivo* therapeutic efficacy**.

Six groups of mice (5 each) were divided as follows: control, liposomal bicarbonate($NaHCO_{3)}$, free doxorubicin(dox), free doxorubicin plus liposomal bicarbonate, liposomal doxorubicin and liposomal doxorubicin (dox) plus liposomal bicarbonate. 50µl of $3x10^5$ cells of 4T1 (triple negative breast cancer) were injected subcutaneously to 8-week-old BALB/c female mice. The mice were weighed and the tumor dimensions were taken three times a week. The tumor volume was measured using a caliper and calculated as ($width^2$xlength)/2. Therapeutic treatment began when the tumor volume reached 100-200mm^3, approximately 10 days after the initial tumor cells injection. The

therapeutic groups: liposomal $NaHCO_3$, free dox and liposomal dox received a single dose each week. In the combined therapy groups, liposomal bicarbonate was injected 24 hours before the injection of free or liposomal dox.

Analysis of different cell populations in tumor tissue.

GentleMacs instrument (Miltenyil Biotec) for dissociation of the extracted tumors was used. Enzyme mix for degradation of the ECM was prepared in the lab as described before. After dissociation the tumor tissue into single cell suspension, cells suspension was incubated with two fluorescent-labeled antibody panels: (1) CD45-FITC, F4/80-BV510, CD19-BV421, CD3-APC and (2) CD-31- BV421, for 20 min in the dark on ice. Ten thousand events were determined for each test sample using LSR BD LSR-II Analyzer (BD Biosciences, New Jersey, USA). Data analysis was performed using FCS Express (De Novo Software, California, USA).

Results and discussion

The acidic pH in the tumor microenvironment is associated with cancer progression, and can lead to drug resistance and consequently to treatment failure [7, 45-47]. In this study alkaline sodium bicarbonate nanoparticles were targeted to murine breast cancer tumors as a mean for enhancing the uptake and potency of the chemically weak-base chemotherapeutic agent – doxorubicin.

Nano drug carriers have been used to promote the pharmacokinetics of medicines towards the disease site and to improve the therapeutic index by protecting delicate biopharmaceuticals from biodegradation and excretion [48]. Rational design of the size and composition of the nanoparticle have been shown to affect the circulation time, volume of distribution, and half-life time in the blood and tumor [31, 49].

Sodium bicarbonate liposomes. PEGylated liposomes, 103.4±27.4nm in diameter, were loaded with sodium bicarbonate as an alkaline buffer (Figure 1A,B). The intra-liposomal pH was evaluated by co-loading sodium bicarbonate with a membrane impermeable pH indicator – pyranine ($excitation_1$=415nm (pH-independent), $excitation_2$=460nm (pH-dependent), emission 510nm) [50]. The intra-liposomal pH of the sodium bicarbonate (50mM) liposomes was 7.8, compared to pH 5.7 in liposomes containing 5% dextrose buffer alone (Figure 1D). This pH remained stable in the liposomes for over one week at 25^{o}C. In addition, to evaluate the contribution of sodium bicarbonate to the pH, a direct measurement of the intra-liposomal aqueous compartment was conducted after removing the liposome lipids using the Bligh and Dyer extraction method (Figure 1E) [51]. This measurement yielded an intra-liposomal aqueous compartment having a slightly higher pH value of 8.2±0.02 (Figure 1E), most likely due to the extraction procedure. The intra-liposomal sodium bicarbonate content was also quantified using ICP elemental analysis of the sodium, to reach a value of 14.5±2.1 mM (Figure S3).

Bicarbonate enhances the uptake and activity of doxorubicin by breast cancer cells. The effect of sodium bicarbonate on the uptake of doxorubicin by triple-negative (4T1) breast cancer cells was studied. Two tissue culture conditions were compared: a) the media

pH was adjusted to 6.5±0.1**,** modeling the acidic tumor microenvironment, or, b) pH 7.4±0.1 to model the normal physiological conditions [3, 7, 9]. The potency of doxorubicin (0.5µg/ml) was greatest when combined with bicarbonate (50mM, Figure 2B). Cells treated with doxorubicin had 48% viability compared to 12% viability in cells treated with doxorubicin plus bicarbonate at an initial media pH of 6.5. At pH 7.4 the effect of bicarbonate was minor (22 vs. 5% viability). The combination of doxorubicin and bicarbonate resulted in an enhanced effect compared to doxorubicin alone. Interestingly, *in vitro*, the effect of free bicarbonate was greater than that of the liposomal bicarbonate, suggesting that optimally the bicarbonate should be released outside the cells (Figure 2B). The enhanced activity of doxorubicin combined with bicarbonate under acidic conditions is attributed to shifting the chemical equilibrium of doxorubicin to its uncharged form, which is favorable for penetrating cell membranes (Figure 2A). Contrarily, at normal physiological pH 7.4, doxorubicin penetrates the cells sufficiently also without bicarbonate.

To further understand the nature of enhanced cytotoxicity obtained using bicarbonate, a HEPES buffer was used as a pH control. Cell viability was examined after treating the cells with doxorubicin combined with HEPES buffer (50mM) compared to doxorubicin alone (Figure 2C). Minor difference was observed between the HEPES plus doxorubicin or doxorubicin alone groups, while the groups treated with doxorubicin plus bicarbonate had greatest potency (Figure 2B vs 2C). Figure 2D and 2E compare between pH values in culture over time, using HEPES (ionic) buffer and bicarbonate. While the HEPES holds a constant buffering capacity, bicarbonate pH increases gradually over time. The difference in activity using HEPES and bicarbonate may be owed to the difference in nature between these two buffers. Bicarbonate, counters the acidic environment through production of $CO_{2(g)}$ which diffuses out of the media to the environment, thereby constantly increasing the pH (Figure 2D,E,G). Contrarily, HEPES, is an ion-based buffer, which creates a stable pH environment, thereby less effective in facilitating doxorubicin uptake (Figure 2C,D,E) [52]. Similar results were obtained using another ionic buffer – BES (N,N-Bis(2-hydroxyethyl)taurine, Figure S4). However, in all these cases the data demonstrate that alkali pH is beneficial for enhancing doxorubicin activity (Figure 2B, C, F, and G).

To further validate the effect of a bicarbonate-induced alkaline environment on the cellular uptake of drugs, we tested its effect on the activity of a chemically neutral anticancer agent (cisplatin, pKa 5.06) and of the weak acid drug 5-fluouracil (5FU, pKa 8.02). In both cases, as expected, the alkaline environment retarded the activity of these drugs (Figure 4A-B). These data corroborate earlier findings that an alkaline pH decreases cisplatin and 5FU activity. Specifically, previous studies have shown that cisplatin activity and side effects increase in an acidic pH due to improved DNA-binding [53-57], where 5-FU behaves as a weak acid, through the ionization of the enolic hydroxyl groups, which inhibits its cellular uptake in alkaline media [7, 58].

To further elucidate the production of CO_2, we imaged triple-negative breast cancer tumors in vivo using ultrasound, before and after administering liposomal bicarbonate (Figure 5D,E). Increased contrast was recorded in the bicarbonate-treated tumors, compared to tumors treated with empty liposomes (Figure 5D- white circle region, 5E). The acidic environment in the tumor catalyzes bicarbonate into CO_2 and water, the CO_2 gas is then detectable by ultrasonic imaging [39, 59-61].

Doxorubicin uptake into cancer cells was visualized using confocal microscopy at two pH conditions: 6.5±0.1 and 7.4±0.1. Breast cancer cells were incubated with doxorubicin in the presence or absence of bicarbonate. Enhanced uptake of doxorubicin (a fluorescent molecule itself) was observed when combined with bicarbonate, compared to the doxorubicin control (Figure 3A). Quantitative flow cytometry analysis indicated a 2.5-fold increase in the doxorubicin uptake by cells treated with doxorubicin plus bicarbonate compared to cells treated with doxorubicin alone at pH 6.5, while the uptake at pH 7.4 was increased by 2-fold (Figure 3B). Image analysis of 10,000 randomly selected 4T1 cells from each treatment group demonstrated increased doxorubicin uptake in the nucleus and cytoplasm of cells treated with doxorubicin plus bicarbonate, compared to cells treated by doxorubicin alone (Figure 3D and S6).

Microscopy-based image analysis depends on the fluorescent signal of doxorubicin inside the cells. However, at high concentrations doxorubicin self-quenches and the fluorescent signal is not indicative of the true drug concentration. To rule out any possible self-quenching of doxorubicin's fluorescent signal inside the cells (which may affect microscopy-based quantifications) [62], we also extracted doxorubicin biochemically from

the cells of each treatment group and quantified the drug independently. These experiments confirmed a 2-fold greater cellular uptake of doxorubicin in the bicarbonate-treated cells versus the untreated control (Figure 3CII). Specifically, doxorubicin concentrations in cells treated with bicarbonate at pH of 6.5 and 7.4 were 0.61µg/ml±0.02 and 0.67µg/ml ±0.06, respectively, while the cellular concentration of doxorubicin without the bicarbonate conditioning was 0.2µg/ml±0.03 and 0.37µg/ml±0.05 (Figure 3CII).

Targeting bicarbonate to orthotopic breast cancer tumors. To test the capacity of the bicarbonate liposomes to target breast cancer tumors *in vivo*, liposomes were loaded with Gadolinium (Gd, a molecular tracer) plus bicarbonate, and injected intravenously to mice bearing orthotopic triple-negative breast cancer (4T1) tumors. The accumulation of liposomal Gd-bicarbonate versus free (non-liposomal) Gd-bicarbonate in the tumor tissue was quantified 24 hours post intravenous administration. Elemental analysis (ICP) of the tissue indicated that 3.7%±0.34 of the injected dose accumulated in the tumor in the liposomal-Gd bicarbonate group, compared to 0.17%±0.04 in the non-liposomal free Gd group. This finding confirms the favorable targeting of PEGylated nano liposomes to the tumor, compared to free bicarbonate molecules injected intravenously.

Inside the tumor, we studied the partition of liposomes between the extracellular matrix (ECM) versus liposomes taken up by the tumor cells. Gd-loaded liposomes were injected intravenously to mice bearing orthotopic triple-negative breast cancer tumors. Twenty-four hours later we resected the tumors and quantified the Gadolinium in the tumor cells and in the ECM. We found that majority (93±1%) of the liposomes were located in the ECM, while only 7±1% of the liposome were taken up by the tumor cells, Figure 5A. Previous studies suggest that the discrepancy between the relatively high accumulation of nanoparticles in solid tumors [63-71], versus the rather comparable therapeutic efficacy to the free drug, suggests that liposomes captured in the extracellular matrix have low bioavailability [71-73]. Several approaches have been employed to improve the bioavailability of drugs loaded into nanoparticles trapped in the extracellular matrix, including using ultrasound [74-81], enzymes [26, 82] or cell-specific surface modifications

such as using monoclonal antibodies, cationic lipids or phospholipid-anchored folate conjugates to facilitate rapid cellular uptake and escape ECM trapping [83-86].

While the main site of bicarbonate activity seems to be in the extracellular matrix, intracellularly, the bicarbonate liposomes may neutralize the endosomal pH, triggering cytosolic release of doxorubicin as well, similarly to the 'proton sponge' theory [87]. Having this said, we believe the dominant mechanism is drug release outside the cell.

Tumor pH. The intra-tumoral pH was measured 24 hr after an intravenous injection of liposomal bicarbonate to BALB/c mice bearing orthotopic triple negative breast cancer tumors. We chose to measure the pH at this time point since the liposomal accumulation has been shown to peak then in the tumor post IV injection [25, 27]. The pH value in the liposomal bicarbonate-treated group was 7.38±0.04 compared to 7.13±0.06 in the untreated tumor (Figure 5). pH measurement of healthy mammary fat pad had a physiological value of 7.46±0.01. These data indicate that liposomal bicarbonate can elevate the tumor pH. Each tumor was measured in three different sites (as mentioned in the Methods section): two peripheral points and one measurement in the tumor core. For the untreated group, the average of all the measurements was 7.13±0.06, while the pH value measured in the tumor core was 6.89±0.03, compared to 7.3±0.04 in the peripheral measurements. These results demonstrate the ability to affect tumor pH using liposomal bicarbonate. While the differences in pH values between the treated and untreated groups may seem minor, the corresponding proton concentration alterations are much more significant and can affect the protonation state of doxorubicin molecules. Using the Hendrson–Hasselblach equation (pKa of doxorubicin is 8.2) [88], the unionized form of doxorubicin is 76% greater at pH 7.38 compared to 7.13, which is reflected by increased cellular uptake of the drug.

Sodium bicarbonate nanoparticles as an adjuvant treatment in vivo. The effect of liposomal bicarbonate on the anti-tumor activity of free and liposomal doxorubicin activity was examined in mice bearing orthotopic 4T1 tumors (Figure 6A). A sub-therapeutic dose of doxorubicin (4 mg/kg-body-weight) was administered in order to evaluate the adjuvant

activity of the nanoparticulate sodium bicarbonate. Mice treated with liposomal doxorubicin combined with liposomal bicarbonate had the best therapeutic outcome compared to all other treatment groups (Figure 6B). Comparing the tumor sizes of all the experimental time-points (1-21 days post treatment) confirmed that mice treated with a sub-therapeutic doxorubicin dose plus bicarbonate had the slowest disease progression compared to mice treated with free (non-liposomal) doxorubicin or with liposomal doxorubicin (Figure 6B).

Postmortem tumor sizing confirmed that the combined treatment of liposomal bicarbonate and doxorubicin (free or liposomal) was superior to all other treatment groups (Figure 6C&G). Three weeks after the treatment (i.e., 36 days from the commencement of the experiment) mice were scanned for the presence of metastases. Interestingly, lung metastases were observed in the untreated and free doxorubicin groups but not in the combined (doxorubicin and bicarbonate) group (Supplementary Figure S1). For future studies, a longer follow up period may be more informative [89, 90].

We propose that the increase of pH generated by the liposomal bicarbonate increased the unionized form of doxorubicin thereby enhancing its cellular uptake and anti-tumor activity. Moreover, pH modification by liposomal bicarbonate can enhance the release of doxorubicin from liposomes, both explaining the improved therapeutic effect we observed [37].

The effect of the combined treatment on the tumor microenvironment immune cell population was also analyzed. The abundance of CD45+ immune cells, CD19+ (B cells), CD3+ (T-cells) or CDF/48+ (macrophages), was examined using quantitative flow cytometry. 1.5-2-fold increase in the total immune cell population (CD45+) was recorded in groups treated with liposomal bicarbonate compared to the other groups (Figure 6D). Moreover, an increase in T cells, B cells and macrophages populations was observed in groups treated with liposomal bicarbonate (Figure 6E-F). This finding suggests that the adjuvant activity of the bicarbonate liposomes is beyond reducing tumor size alone, and affecting the tumor microenvironment as well. The endothelial cell population was not affected by either of the treatments. Recently, several studies demonstrated a correlation between the acidic tumor pH environment and immunosuppression [91-94]. Antitumor

effectors such as *interferon gamma* (INFg) lose their function at acidic pH [91, 93, 95]. Moreover, modification of the tumor acidic microenvironment by bicarbonate inhibited the growth and progression of several murine tumors [11, 93], this effect was attributed to increased T-cell infiltration [93]. Additionally, a combined treatment of bicarbonate and cancer immunotherapies such as immune checkpoint blockade (anti-CTLA-4, anti-PD1) or adoptive T-cell transfer (ACT) enhanced the anti-tumor responses [93, 95]. Autophagy is one of the ways cancer cells use to prolonged survival in the acidic tumor microenvironment, using bicarbonate pro-autophagy signals were diminished [95]. These results warrant further investigation regarding the capacity of bicarbonate alone to act as a therapeutic modulator of the tumor microenvironment.

The administration of free sodium bicarbonate through the systemic circulation raises safety concerns through the development of metabolic alkalosis and hypernatremia [3, 11]. Having this said, bicarbonate has been suggested to counter the acidic tumor microenvironment [3, 4, 7, 8, 11, 96]. Mathematical diffusion models show that orally administered bicarbonate cannot counteract the acid load in tumors [4]. For this reason, nanoparticle-targeted delivery of sodium bicarbonate can increase bicarbonate accumulation in the tumor tissue while decreasing the risks of adverse effects and toxicity.

Herein, bicarbonate nanoparticles were demonstrated as an effective adjuvant treatment. We found that nanoscale liposomes increase the accumulation of bicarbonate in the tumor tissue. When combined with doxorubicin, bicarbonate supported cellular uptake of the drug and improved the therapeutic efficacy. Combined treatment using an adjuvant may enable lowering drug doses by enhancing the uptake of the available drug. This study aims to show the feasibility of a combined treatment using targeted bicarbonate and doxorubicin nanoparticles, future studies should be conducted to study the effect of bicarbonate for overcoming drug-resistance, by enhancing cellular drug penetration. This work showed that nanotechnology holds great potential as an adjuvant treatment for conditioning the tumor microenvironment towards improved drug activity.

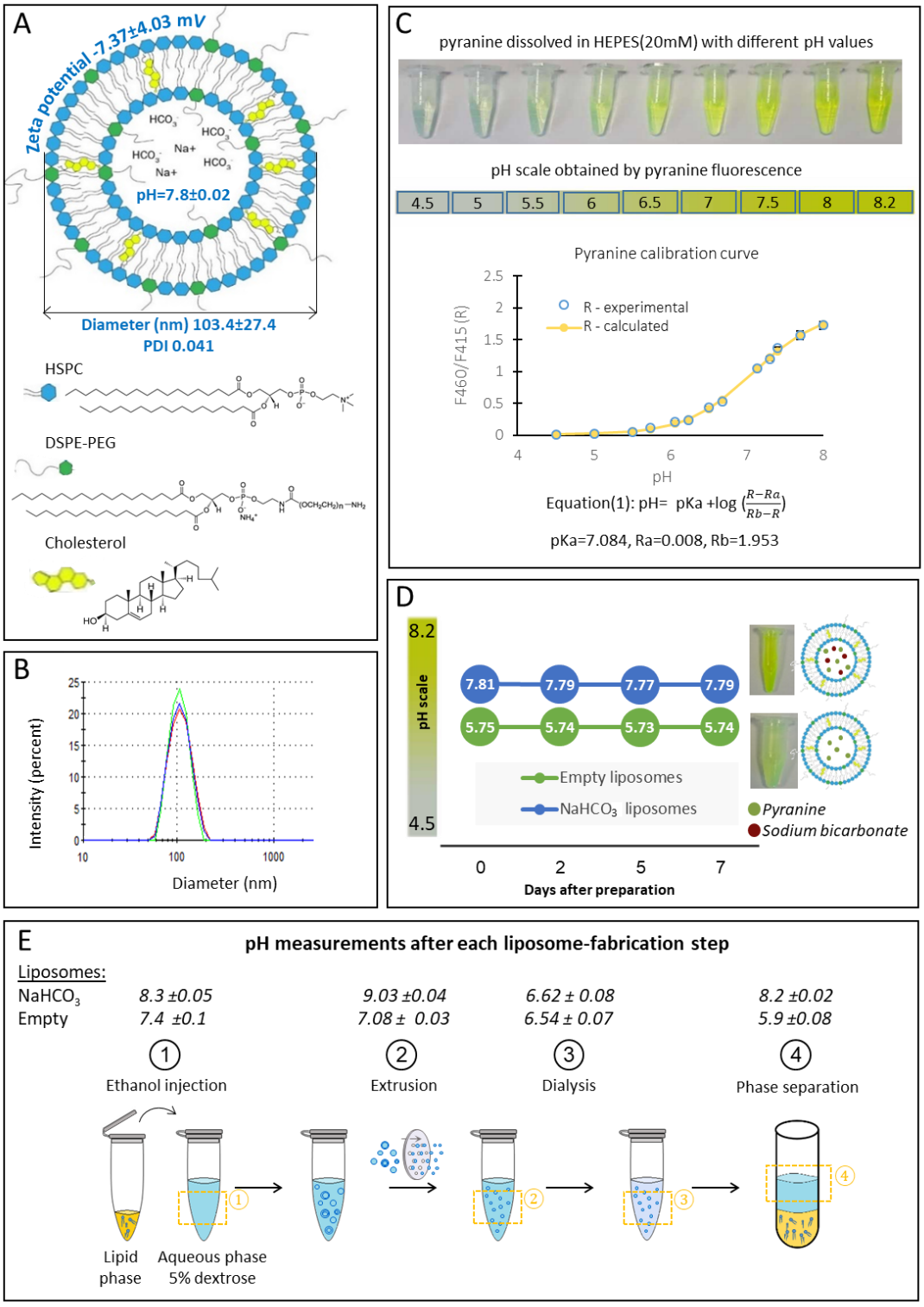

506

507 **Figure 1: Sodium bicarbonate nanoparticles.** Liposomes encapsulating sodium bicarbonate were
508 constructed of HSPC, cholesterol and PEG-DSPE at 50mM total lipid concentration (A) having a mean
509 diameter of 103nm (B), and a zeta potential of -7.37mV (A). The intra-liposomal pH was 7.8±0.02, measured

using a pyranine indicator (C-D). Intra-liposomal pH measurements over time showed stable values over one week (25 ^{o}C). (E steps1-3) Direct pH measurements of the aqueous phase after being extracted during the liposome formulation process. (E step4) Normalized pH of the aqueous phase after Bligh and Dyer phase separation.

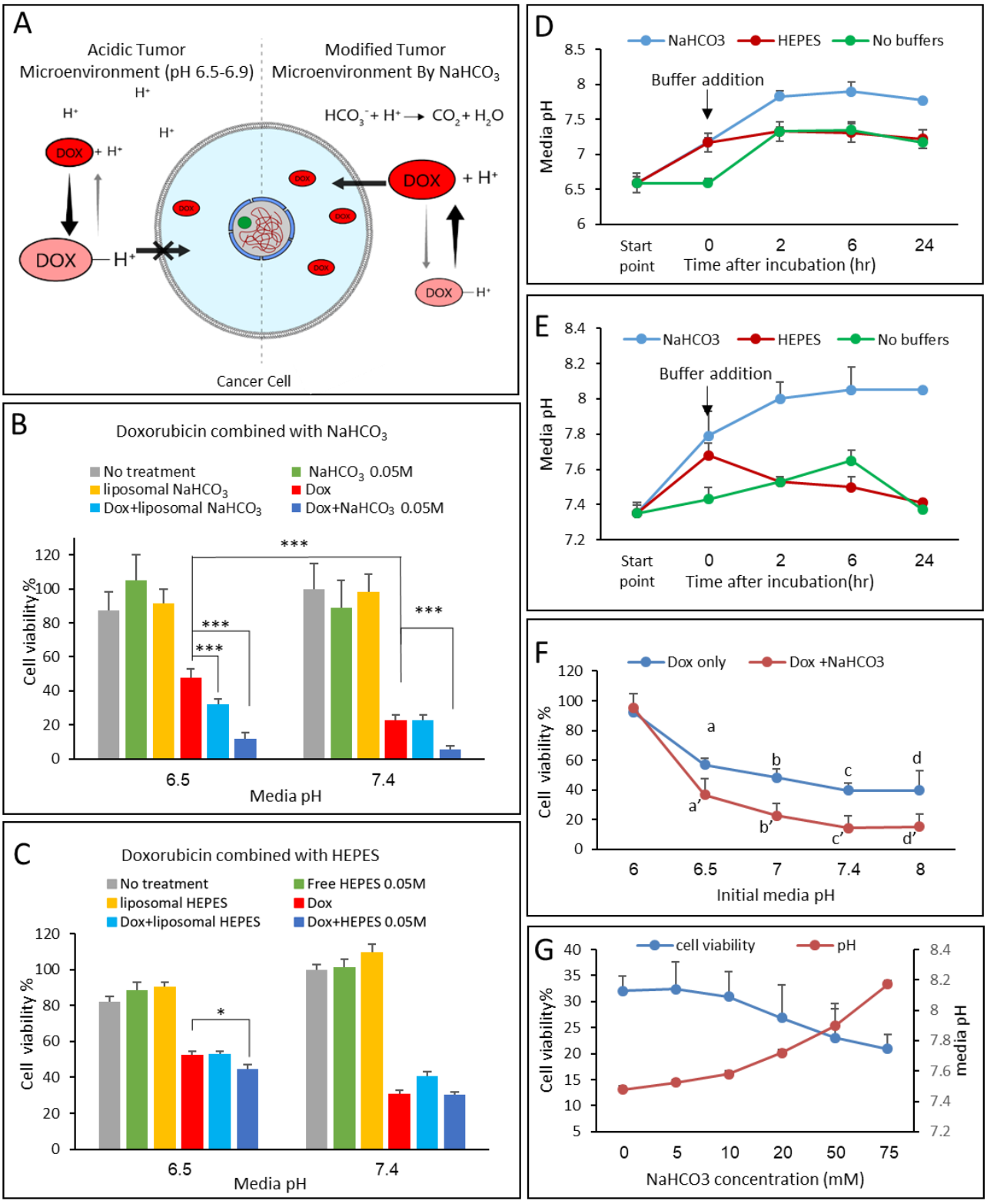

Figure 2: Bicarbonate enhances the activity of doxorubicin in 4T1 breast cancer cells. (A) A schematic representation of the mechanism of doxorubicin uptake by cancer cells in acidic and neutral environments. (B+C) Cell viability was measured in representative physiological (7.4) and cancerous (6.5) pH. Doxorubicin

518 (0.5µg/ml) with and without sodium bicarbonate (50mM), or HEPES, was added to cancer cells in culture,
519 and cell viability was measured after 24 hours. (D+E) measurement of cell media pH change throughout the
520 experiments. (F) Doxorubicin effect on cells' viability with and without $NaHCO_3$ (50mM). a and a' indicate
521 $p<0.05$ while significant differences between groups b to b', c to c', d to d' had $p<0.01$. (G) Cell viability
522 (left axis) after treatment with different concentrations of $NaHCO_3$ (5-75mM) combined with doxorubicin,
523 statistical significance (**p<0.01). Right axis presents media pH measurements during the experiment.

524 Error bars represent standard deviation from 3 to 5 independent repeats. *Significant difference between
525 treatments, where *p<0.05, **p<0.01, ***p<0.001 according to a Student's t-test with a two-tailed
526 distribution with equal variance.

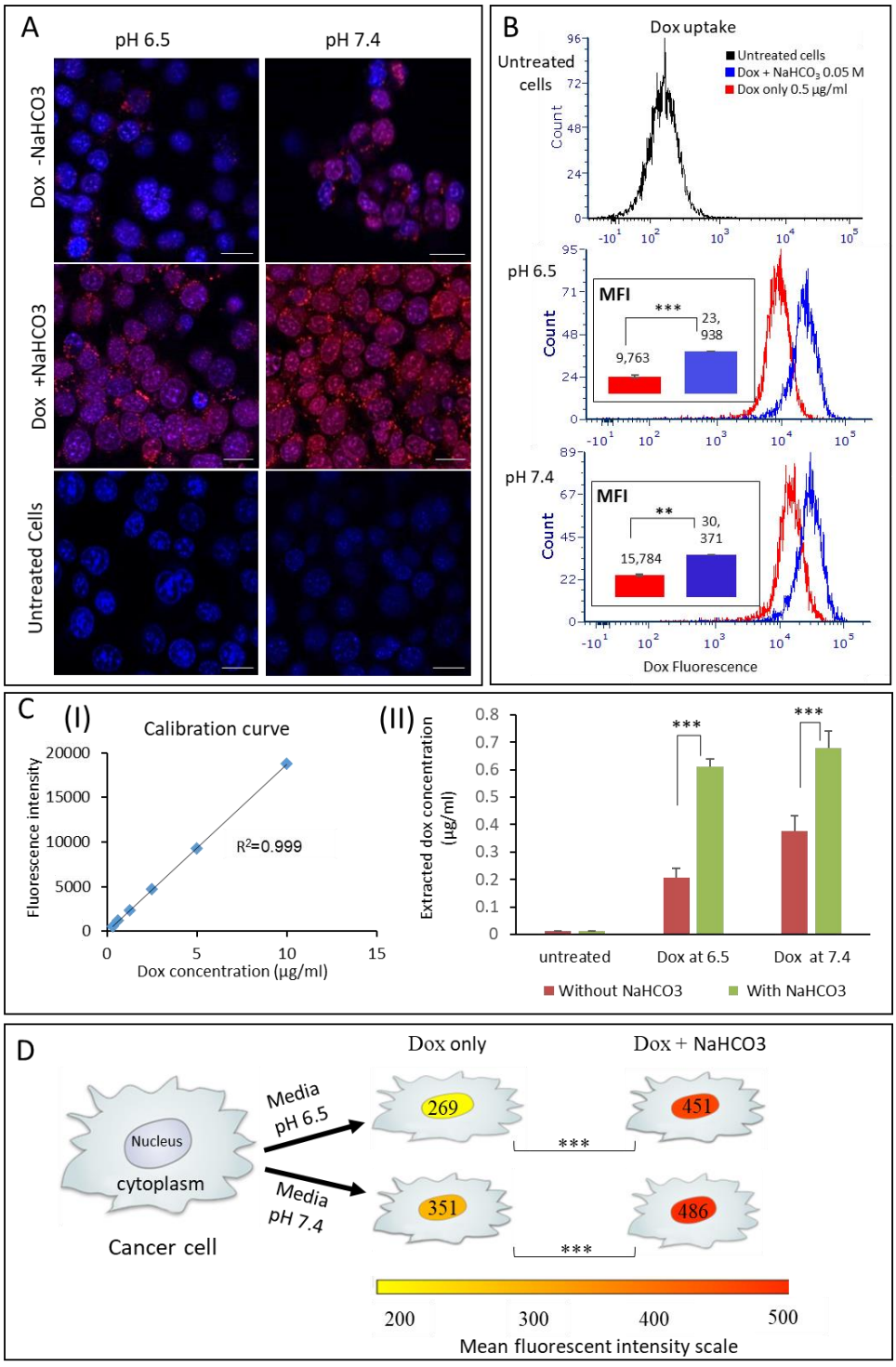

Figure 3: Bicarbonate enhances the uptake of doxorubicin by 4T1 breast cancer cells. (A) Increased cellular uptake of doxorubicin (red) can be seen using fluorescent microscopy after adding bicarbonate to the culture, compared to doxorubicin uptake without bicarbonate. Cell nucleus is stained blue. (B) Quantifying doxorubicin uptake using flow cytometry indicated a right-shift in the histogram of cells treated with

combined treatment (blue histogram) representing a 2-fold increase in doxorubicin uptake when combined with bicarbonate. MFI represents the mean fluorescence intensity. (C) Doxorubicin concentrations after being extracted from the cells (II) with or without bicarbonate; concentrations were determined based on calibration curve of the drug dissolved in methanol (I). (D) Quantification of doxorubicin fluorescent intensity in the cell' nuclei, measured using image analysis of more than 10,000 cells in each group. Scale bars in (A) represent 20µm; error bars represent standard deviation from 3 to 5 independent repeats. *Significant difference between treatments, where *p<0.05, **p<0.01, ***p<0.001 according to a Student's *t*-test with a two-tailed distribution with equal variance.

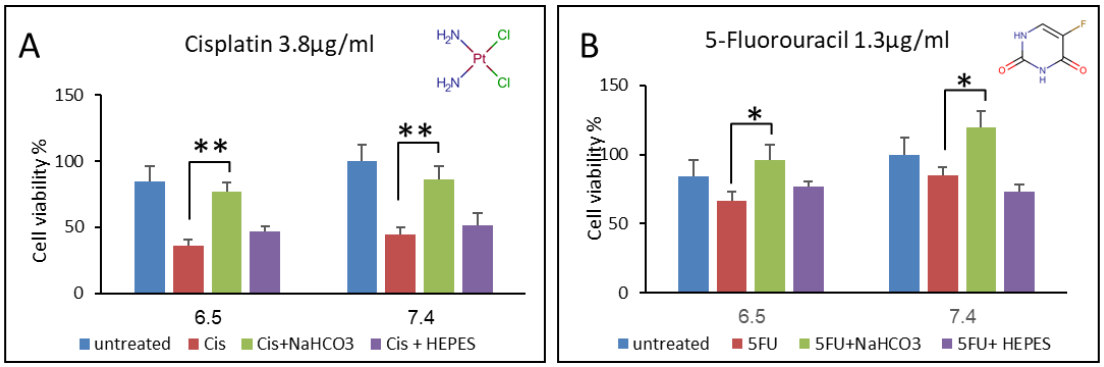

C

Chemotherapeutic agent	Effect after combination with $NaHCO_3$(50mM)	
	Increased activity	*Decreased activity*
Doxorubicin	*V*	
Cisplatin		*V*
5-Fluorouracil		*V*

Figure 4: Combined treatment of bicarbonate and different chemotherapeutic agents: (A+B) Cisplatin (pKa 5.06, 3.8µg/ml) and 5-fluorouracil (5FU, pKa 8.02, 1.3µg/ml) effect on 4T1 breast cancer cells after combination with bicarbonate (50mM) and HEPES buffer (50mM). (C) Summary of bicarbonate effect on chemotherapeutic agents' activity on 4T1 cells after a combined treatment.

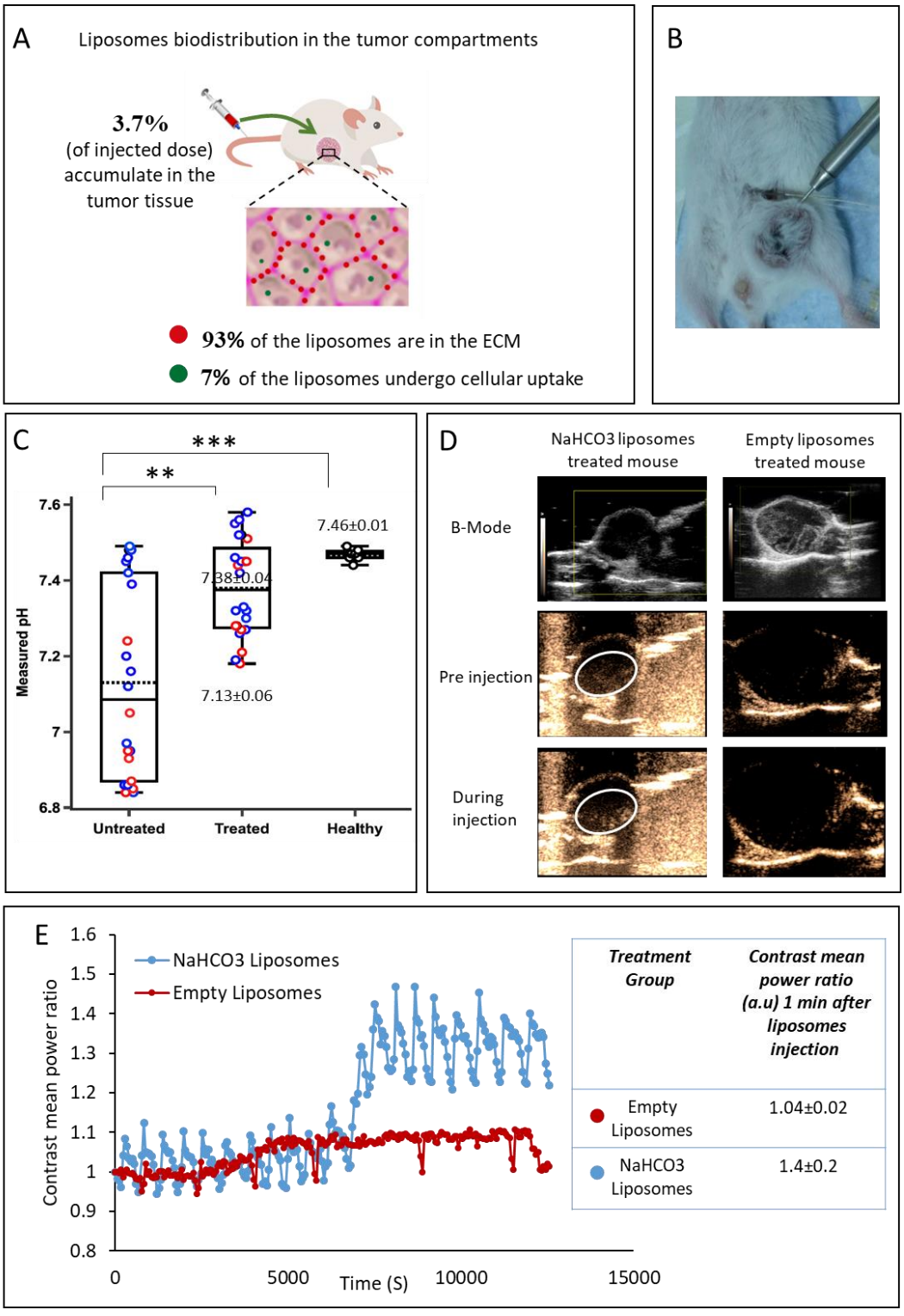

Figure 5: Bicarbonate liposomes effect in the tumor microenvironment. (A) Bicarbonate liposomes biodistribution in the cells and extracellular matrix (ECM) of orthotopic triple-negative tumors 24 hours after intravenous injection. (B+C) In vivo pH measurements of the tumor and healthy tissue. The intra-tumoral pH was measured using microelectrodes 24-hr after administering bicarbonate liposomes (B). Treated tumors

with liposomal bicarbonate modified the pH in the tumor tissue after IV injection, compared to untreated mice(C). Red circles represent pH tumor core measurements while the blue represent peripheral ones. 7.13±0.06 and 7.38±0.04 represent the averaged pH of all measurements in the untreated and treated groups respectively. pH of healthy mammary fat pad was found to be in the physiologic range, 7.46±0.01. Error bars represent standard deviation of the mean from 5-7 independent repeats. *Significant difference between treatments, where *$p<0.05$, **$p<0.01$, ***$p<0.001$according to a Student's t-test with a two-tailed distribution with equal variance. (D) Breast cancer tumors ultrasound scanning before and during the injection of bicarbonate or empty liposomes. B-mode images present the tumor. Before and during the injection, images were taken using contrast-mode. (E) Contrast mean power ratio measures the change in the contrast during liposomes injection, blue curve represents bicarbonate liposomes and the red curve represents empty liposomes. The contrast means power ratios 1 min after the liposomes injection (compared to pre injection) were 1.41±0.2(n=3) and 1.04±0.02(n=3) for $NaHCO_3$ liposomes and empty liposomes respectively (p value=0.08).

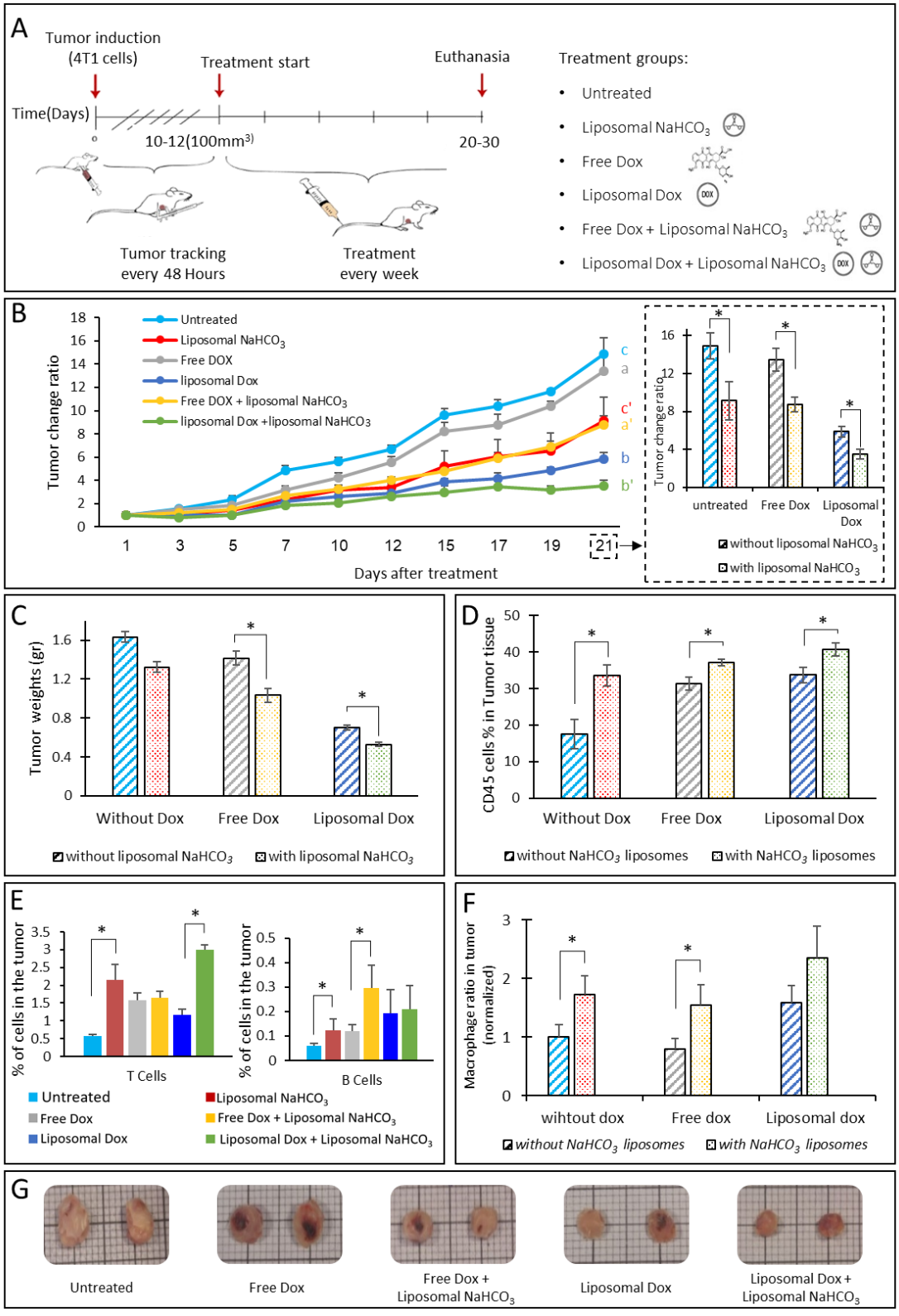

564

565 **Figure 6: Liposomal bicarbonate increases doxorubicin efficacy in breast cancer**. The effect of
566 liposomal bicarbonate as an adjuvant for enhancing doxorubicin activity in-vivo, was studied (A). Once

tumors reached 100-200mm^3 treatments began, using free doxorubicin(dox) (4 mg/kg-body-weight), liposomal doxorubicin (4 mg/kg) and a combination of the two with liposomal $NaHCO_3$. Tumors were sized every other day. In all the time points, for each mouse the tumor size was normalized to the initial size measured at day 1(B), a and a' show statistical differences($p<0.05$) after 12 days and continued through the last time point (21 days), statistical differences($p<0.05$) between b and b' were observed later, in the last two measurements. For c and c' differences were observed after 10 days ($p<0.05$). At the end of the experiments tumors were extracted, weighed and imaged (C and G). An increase in total immune cell (CD45+), T cells (CD3+), B cells (CD19+) and macrophages(CDF/48+) populations in the tumor tissue was also observed in the treatment groups (D-F). (F) Macrophages ratio in the tumor tissue normalized to untreated group. Error bars represent standard deviation of the mean from 4 to 5 independent repeats. *Significant difference between treatments, where *$p<0.05$, according to a Student's t-test with a two-tailed distribution with equal variance.

Acknowledgments

This work was supported by ERC-STG-2015-680242.

The authors also acknowledge the support of the Technion Integrated Cancer Center (TICC), the Russell Berrie Nanotechnology Institute, the Lorry I. Lokey Interdisciplinary Center for Life Sciences & Engineering, the Pre-Clinical Research Authority staff and the Biomedical Core Facility at the Rappaport Faculty of Medicine, as well as the Israel Ministry of Economy for a Kamin Grant (52752); the Israel Ministry of Science Technology and Space – Office of the Chief Scientist (3-11878); the Israel Science Foundation (1778/13, 1421/17); the Israel Cancer Association (2015-0116); the German-Israeli Foundation for Scientific Research and Development for a GIF Young grant (I-2328-1139.10/2012); the European Union FP-7 IRG Program for a Career Integration Grant (908049); the Phospholipid Research Center Grant; a Mallat Family Foundation Grant; The Unger Family Fund; A. Schroeder acknowledges Alon and Taub Fellowships. A. Zinger acknowledges a generous fellowship form the Technion Russell Berrie Nanotechnology Institute (RBNI). N. Krinsky and H. Abumanhal wish to thank the Baroness Ariane de Rothschild Women Doctoral Program for its generous support.

References

[1]K.M. Skubitz, Phase II trial of pegylated-liposomal doxorubicin (Doxil) in renal cell cancer, Investigational new drugs, 20 (2002) 101-104.

[2]T.L. ten Hagen, A.L. Seynhaeve, S.T. van Tiel, D.J. Ruiter, A.M. Eggermont, Pegylated liposomal tumor necrosis factor-alpha results in reduced toxicity and synergistic antitumor activity after systemic administration in combination with liposomal doxorubicin (Doxil) in soft tissue sarcoma-bearing rats, International journal of cancer, 97 (2002) 115-120.

[3]V. Estrella, T. Chen, M. Lloyd, J. Wojtkowiak, H.H. Cornnell, A. Ibrahim-Hashim, K. Bailey, Y. Balagurunathan, J.M. Rothberg, B.F. Sloane, J. Johnson, R.A. Gatenby, R.J. Gillies, Acidity generated by the tumor microenvironment drives local invasion, Cancer research, 73 (2013) 1524-1535.

[4]I.F. Robey, B.K. Baggett, N.D. Kirkpatrick, D.J. Roe, J. Dosescu, B.F. Sloane, A.I. Hashim, D.L. Morse, N. Raghunand, R.A. Gatenby, R.J. Gillies, Bicarbonate increases tumor pH and inhibits spontaneous metastases, Cancer research, 69 (2009) 2260-2268.

[5]J.W. Wojtkowiak, D. Verduzco, K.J. Schramm, R.J. Gillies, Drug resistance and cellular adaptation to tumor acidic pH microenvironment, Molecular pharmaceutics, 8 (2011) 2032-2038.

[6]L.E. Gerweck, S. Vijayappa, S. Kozin, Tumor pH controls the in vivo efficacy of weak acid and base chemotherapeutics, Molecular cancer therapeutics, 5 (2006) 1275-1279.

[7]Y. Kato, S. Ozawa, C. Miyamoto, Y. Maehata, A. Suzuki, T. Maeda, Y. Baba, Acidic extracellular microenvironment and cancer, Cancer cell international, 13 (2013) 89.

[8]B.P. Mahoney, N. Raghunand, B. Baggett, R.J. Gillies, Tumor acidity, ion trapping and chemotherapeutics. I. Acid pH affects the distribution of chemotherapeutic agents in vitro, Biochemical pharmacology,.1207-1218 (2003) 66

[9]N. Raghunand, X. He, R. van Sluis, B. Mahoney, B. Baggett, C.W. Taylor, G. Paine-Murrieta, D. Roe, Z.M. Bhujwalla, R.J. Gillies, Enhancement of chemotherapy by manipulation of tumour pH, British journal of cancer, 80 (1999) 1005-.1011

[10]T. Yoneda, M. Hiasa, Y. Nagata, T. Okui, F. White, Contribution of acidic extracellular microenvironment of cancer-colonized bone to bone pain, Biochimica et biophysica acta, 1848 (2015) 2677-2684.

[11]S. Faes, O. Dormond, Systemic Buffers in Cancer Therapy: The Example of Sodium Bicarbonate; Stupid Idea or Wise Remedy?, Medicinal Chemistry, 5 (2015).

[12]A.S. Silva, J.A. Yunes, R.J. Gillies, R.A. Gatenby, The potential role of systemic buffers in reducing intratumoral extracellular pH and acid-mediated invasion, Cancer research, 69 (2009) 2677-2684.

[13]T.J. Berg JM, Stryer L, Biochemistry. 5th edition,Section 9.2, Making a Fast Reaction Faster: Carbonic Anhydrases, 2002,New York: W H Freeman.

[14]M. Zatovicova, L. Jelenska, A. Hulikova, L .Csaderova, Z. Ditte, P. Ditte, T. Goliasova, J. Pastorek, S. Pastorekova, Carbonic Anhydrase IX as an Anticancer Therapy Target: Preclinical Evaluation of Internalizing Monoclonal Antibody Directed to Catalytic Domain, Current Pharmaceutical Design, 16 .3255-3263 (2010)

[15]A.S. Betof, Z.N. Rabbani, M.E. Hardee, S.J. Kim, G. Broadwater, R.C. Bentley, S.A. Snyder, Z. Vujaskovic, E. Oosterwijk, L.N. Harris, J.K. Horton, M.W. Dewhirst, K.L. Blackwell, Carbonic anhydrase IX is a predictive marker of doxorubicin resistance in early-stage breast cancer independent of HER2 and TOP2A amplification, British journal of cancer, 106 (2012) 916-922.

[16]M.L. Etheridge, S.A. Campbell, A.G. Erdman, C.L. Haynes, S.M. Wolf, J. McCullough, The big picture on nanomedicine: the state of investigational and approved nanomedicine products, Nanomedicine, 9 (2013) 1-14.

[17]A. Hafner, J. Lovric, G.P. Lakos, I. Pepic, Nanotherapeutics in the EU: an overview on current state and future directions, Int J Nanomedicine, 9 (2014).1005-1023
[18]V. Weissig, D. Guzman-Villanueva, Nanopharmaceuticals (part 2): products in the pipeline, Int J Nanomedicine, 10 (2015) 1245-1257.
[19]V. Weissig, T.K. Pettinger, N. Murdock, Nanopharmaceuticals (part 1): products on the market, Int J Nanomedicine, 9 (2014) 4357-4373.
[20]C.W. Noorlander, M.W. Kooi, A.G. Oomen, M.V. Park, R.J. Vandebriel, R.E. Geertsma, Horizon scan of nanomedicinal products, Nanomedicine (Lond), 10 (2015) 1599-1608.
[21]P. Evers, Nanotechnology in Medical Applications :The Global Market, in: Healthcare Market Research Reports, BCC Research, 2015.
[22]R. Duncan, R. Gaspar, Nanomedicine(s) under the microscope, Mol Pharm, 8 (2011) 2101-2141.
[23]W.J. Stark, Nanoparticles in biological systems, Angewandte Chemie, 50 (.1242-1258 (2011
[24]V.P. Torchilin, Multifunctional, stimuli-sensitive nanoparticulate systems for drug delivery, Nat Rev Drug Discov, 13 (2014) 813-827.
[25]E. Goldman, A. Zinger, D. da Silva, Z. Yaari, A. Kajal, D. Vardi-Oknin, M. Goldfeder, J.E. Schroeder, J. Shainsky-Roitman, D. Hershkovitz, A. Schroeder, Nanoparticles target early-stage breast cancer metastasis in vivo, Nanotechnology, 28 (2017) 43LT01.
[26]A. Zinger, O. Adir, M. Alper, A. Simon, M. Poley, C. Tzror, Z. Yaari, M. Krayem, S. Kasten ,G. Nawy, A. Herman, Y. Nir, S. Akrish, T. Klein, J. Shainsky-Roitman, D. Hershkovitz, A. Schroeder, Proteolytic Nanoparticles Replace a Surgical Blade by Controllably Remodeling the Oral Connective Tissue, ACS Nano, (2018).
[27]Z. Yaari, D. da Silva, A .Zinger, E. Goldman, A. Kajal, R. Tshuva, E. Barak, N. Dahan, D. Hershkovitz, M. Goldfeder, J.S. Roitman, A. Schroeder, Theranostic barcoded nanoparticles for personalized cancer medicine, Nat Commun, 7 (2016) 13325.
[28]H. Maeda, Y. Matsumura, EPR effect based drug design and clinical outlook for enhanced cancer chemotherapy Preface, Advanced Drug Delivery Reviews, 63 (2011) 129-130.
[29]J. Folkman, Can mosaic tumor vessels facilitate molecular diagnosis of cancer?, Proc Natl Acad Sci U S A, 98 (2001).398-400
[30]V.P. Chauhan, T. Stylianopoulos, J.D. Martin, Z. Popovic, O. Chen, W.S. Kamoun, M.G. Bawendi, D. Fukumura, R.K. Jain, Normalization of tumour blood vessels improves the delivery of nanomedicines in a size-dependent manner, Nat Nanotechnol, .383-388 (2012) 7
[31]B. Aslan, B. Ozpolat, A.K. Sood, G. Lopez-Berestein, Nanotechnology in cancer therapy, Journal of drug targeting, 21 (2013) 904-913.
[32]G. Zhao, B.L. Rodriguez, Molecular targeting of liposomal nanoparticles to tumor microenvironment, International journal of nanomedicine, 8 (2013) 61-71.
[33]T. Ojha, L. Rizzo, G. Storm, F. Kiessling, T. Lammers, Image-guided drug delivery: preclinical applications and clinical translation, Expert opinion on drug delivery, 12 (2015) 1203-1207.
[34]B. Theek, F. Gremse, S. Kunjachan, S. Fokong, R. Pola, M. Pechar, R. Deckers, G. Storm, J. Ehling, F. Kiessling, T. Lammers, Characterizing EPR-mediated passive drug targeting using contrast-enhanced functional ultrasound imaging, Journal of controlled release : official journal of the Controlled Release Society, 182 (2014) 83-89.
[35]Y. Barenholz, Nanomedicine: Shake up the drug containers, Nat Nanotechnol, 7 (2012) 483-484.
[36]Y. Barenholz, Doxil(R)--the first FDA-approved nano-drug: lessons learned, J Control Release, 160 (2012) 117-134.

688 [37]L. Silverman, Y. Barenholz, In vitro experiments showing enhanced release of doxorubicin
689 from Doxil(R) in the presence of ammonia may explain drug release at tumor site, Nanomedicine,
690 11 (2015) 1841-1850.
691 [38]K.J. Harrington, S. Mohammadtaghi, P.S. Uster, D. Glass, A.M. Peters, R.G. Vile, J.S. Stewart,
692 Effective targeting of solid tumors in patients with locally advanced cancers by radiolabeled
693 pegylated liposomes, Clin Cancer Res, 7 (2001) 243-254.
694 [39]J. Xia, G. Feng, X. Xia, L. Hao, Z. Wang, NH4HCO3 gas-generating liposomal nanoparticle for
695 photoacoustic imaging in breast cancer, International journal of nanomedicine, 12 (2017) 1803-
696 1813.
697 [40]A. Som, R. Raliya, L. Tian, W. Akers, J.E. Ippolito, S. Singamaneni, P. Biswas, S. Achilefu,
698 Monodispersed calcium carbonate nanoparticles modulate local pH and inhibit tumor growth in
699 vivo, Nanoscale, 8 (2016) 12639-12647.
700 [41]G. Haran, R. Cohen, L.K. Bar, Y. Barenholz, Transmembrane ammonium sulfate gradients in
701 liposomes produce efficient and stable entrapment of amphipathic weak bases, Biochimica et
702 biophysica acta, 1151 (1993) 201-215.
703 [42]Y. Avnir, Y. Barenholz, pH determination by pyranine: medium-related artifacts and their
704 correction, Analytical biochemistry, 347 (2005) 34-41.
705 [43]E.G. Bligh, W.J. Dyer, A rapid method of total lipid extraction and purification, Canadian
706 journal of biochemistry and physiology, 37 (1959) 911-917.
707 [44]A. Andersen, D.J. Warren, L. Slørdal, Quantition of cell-associated doxorubicin by high-
708 performance liquid chromatography after enzymatic desequestration, Cancer chemotherapy and
709 pharmacology, 34 (1994) 197-202.
710 [45]R. Straussman, T. Morikawa, K. Shee, M. Barzily-Rokni, Z.R. Qian, J. Du, A. Davis, M.M.
711 Mongare, J. Gould, D.T. Frederick, Z.A. Cooper, P.B. Chapman, D.B. Solit, A. Ribas, R.S. Lo, K.T.
712 Flaherty, S. Ogino, J.A. Wargo, T.R. Golub, Tumour micro-environment elicits innate resistance to
713 RAF inhibitors through HGF secretion, Nature, 487 (2012) 500-504.
714 [46]M. Upreti, A. Jyoti, P. Sethi, Tumor microenvironment and nanotherapeutics, Translational
715 cancer research, 2 (2013) 309-319.
716 [47]N. Weizman, Y. Krelin, A. Shabtay-Orbach, M. Amit, Y. Binenbaum, R.J. Wong, Z. Gil,
717 Macrophages mediate gemcitabine resistance of pancreatic adenocarcinoma by upregulating
718 cytidine deaminase, Oncogene, 33 (2014) 3812-3819.
719 [48]P.R. Cullis, M.J. Hope, Lipid Nanoparticle Systems for Enabling Gene Therapies, Mol Ther, 25
720 (2017) 1467-1475.
721 [49]S.D. Li, L. Huang, Pharmacokinetics and biodistribution of nanoparticles, Molecular
722 pharmaceutics, 5 (2008) 496-504.
723 > [50]Pyranine (8-Hydroxy- 1,3,6-pyrenetrisulfonate) as a Probe of Internal Aqueous.pdf>.
724 [51]E.G. Bligh, W.J. Dyer, A rapid method of total lipid extraction and purification, Can. J. Biochem.
725 Physiol., 37 (1959) 911-917.
726 [52]Y. Barenholz, D.D. Lasic, Handbook of Nonmedical Applications of Liposomes, Taylor &
727 Francis, 1996.
728 [53]A. Atema, K.J. Buurman, E. Noteboom, L.A. Smets, Potentiation of DNA-adduct formation and
729 cytotoxicity of platinum-containing drugs by low pH, International journal of cancer, 54 (1993)
730 166-172.
731 [54]F. Tanaka, C.A. Whitworth, L.P. Rybak, Influence of pH on the ototoxicity of cisplatin: a round
732 window application study, Hearing Research, 177 (2003) 21-31.
733 [55]J. Guindon, A.G. Hohmann, Use of sodium bicarbonate to promote weight gain, maintain
734 body temperature, normalize renal functions and minimize mortality in rodents receiving the
735 chemotherapeutic agent cisplatin, Neuroscience letters, 544 (2013) 41-46.

[56]E. Groos, L. Walker, J.R.W. Masters, Intravesical chemotherapy: Studies on the relationship between ph and cytotoxicity, Cancer, 58 (1986) 1199-1203.
[57]T. Murakami, I. Shibuya, T. Ise, Z.S. Chen, S. Akiyama, M. Nakagawa, H. Izumi, T. Nakamura, K. Matsuo, Y. Yamada, K. Kohno, Elevated expression of vacuolar proton pump genes and cellular PH in cisplatin resistance, International journal of cancer, 93 (2001) 869-874.
[58]A.S. Ojugo, P.M. McSheehy, M. Stubbs, G. Alder, C.L. Bashford, R.J. Maxwell, M.O. Leach, I.R. Judson, J.R. Griffiths, Influence of pH on the uptake of 5-fluorouracil into isolated tumour cells, British journal of cancer, 77 (1998) 873-879.
[59]K. Zhang, H. Xu, H. Chen, X. Jia, S. Zheng, X. Cai, R. Wang, J. Mou, Y. Zheng, J. Shi, CO2 bubbling-based 'Nanobomb' System for Targetedly Suppressing Panc-1 Pancreatic Tumor via Low Intensity Ultrasound-activated Inertial Cavitation, Theranostics, 5 (2015) 1291-1302.
[60]M.-F. Chung, K.-J. Chen, H.-F. Liang, Z.-X. Liao, W.-T. Chia, Y. Xia, H.-W. Sung, A Liposomal System Capable of Generating CO2 Bubbles to Induce Transient Cavitation, Lysosomal Rupturing, and Cell Necrosis, Angewandte Chemie International Edition, 51 (2012) 10089-10093.
[61]K.-J. Chen, H.-F. Liang, H.-L. Chen, Y. Wang, P.-Y. Cheng, H.-L. Liu, Y. Xia, H.-W. Sung, A Thermoresponsive Bubble-Generating Liposomal System for Triggering Localized Extracellular Drug Delivery, ACS nano, 7 (2013) 438-446.
[62]R.J. Lee, P.S. Low, Folate-mediated tumor cell targeting of liposome-entrapped doxorubicin in vitro, Biochim Biophys Acta, 1233 (1995) 134-144.
[63]Y. Matsumura, H. Maeda, A New Concept for Macromolecular Therapeutics in Cancer Chemotherapy: Mechanism of Tumoritropic Accumulation of Proteins and the Antitumor Agent Smancs, Cancer research, 46 (1986) 6387.
[64]Y. Noguchi, J. Wu, R. Duncan, J. Strohalm, K. Ulbrich, T. Akaike, H. Maeda, Early phase tumor accumulation of macromolecules: a great difference in clearance rate between tumor and normal tissues, Japanese journal of cancer research : Gann, 89 (1998) 307-314.
[65]K.S. Ho, A.M. Aman, R.S. Al-awar, M.S. Shoichet, Amphiphilic micelles of poly(2-methyl-2-carboxytrimethylene carbonate-co-D,L-lactide)-graft-poly(ethylene glycol) for anti-cancer drug delivery to solid tumours, Biomaterials, 33 (2012) 2223-2229.
[66]A.A. Gabizon, Selective Tumor Localization and Improved Therapeutic Index of Anthracyclines Encapsulated in Long-Circulating Liposomes, Cancer research, 52 (1992) 891.
[67]S.K. Huang, E. Mayhew, S. Gilani, D.D. Lasic, F.J. Martin, D. Papahadjopoulos, Pharmacokinetics and Therapeutics of Sterically Stabilized Liposomes in Mice Bearing C-26 Colon Carcinoma, Cancer research, 52 (1992) 6774.
[68]R. Weissleder, K. Kelly, E.Y. Sun, T. Shtatland, L. Josephson, Cell-specific targeting of nanoparticles by multivalent attachment of small molecules, Nature Biotechnology, 23 (2005) 1418.
[69]P. Puvanakrishnan, J. Park, D. Chatterjee, S. Krishnan, J.W. Tunnell, In vivo tumor targeting of gold nanoparticles: effect of particle type and dosing strategy, International journal of nanomedicine, 7 (2012) 1251-1258.
[70]K.J. Harrington, S. Mohammadtaghi, P.S. Uster, D. Glass, A.M. Peters, R.G. Vile, J.S.W. Stewart, Effective Targeting of Solid Tumors in Patients With Locally Advanced Cancers by Radiolabeled Pegylated Liposomes, Clinical Cancer Research, 7 (2001) 243.
[71]K.M. Laginha, S. Verwoert, G.J.R. Charrois, T.M. Allen, Determination of Doxorubicin Levels in Whole Tumor and Tumor Nuclei in Murine Breast Cancer Tumors, Clinical Cancer Research, 11 (2005) 6944.
[72]T. Lammers, F. Kiessling, M. Ashford, W. Hennink, D. Crommelin, G. Storm, Cancer nanomedicine: Is targeting our target?, Nature reviews. Materials, 1 (2016) 16069.

783 [73]E. Blanco, H. Shen, M. Ferrari, Principles of nanoparticle design for overcoming biological
784 barriers to drug delivery, Nature biotechnology, 33 (2015) 941-951.
785 [74]G.G. Dimcevski, S. Kotopouli, T. Bjåne, D. Hoem, J. Schjött, B.T. Gjertsen, M. Biermann, A.
786 Molven, H. Sorbye, E. McCormac, M. Postema, O.H. Gilja, Ultrasound and microbubble enhanced
787 treatment of inoperable pancreatic adeonocarcinoma, Journal of Clinical Oncology, 34 (2016)
788 e15703-e15703.
789 [75]S. Kotopoulis, A. Delalande, M. Popa, V. Mamaeva, G. Dimcevski, O.H. Gilja, M. Postema, B.T .
790 Gjertsen, E. McCormack, Sonoporation-Enhanced Chemotherapy Significantly Reduces Primary
791 Tumour Burden in an Orthotopic Pancreatic Cancer Xenograft, Molecular Imaging and Biology, 16
792 (2014) 53-62.
793 [76]A.v. Wamel, A. Healey, P.C. Sontum, S. Kvåle, N. Bush, J. Bamber, C. de Lange Davies, Acoustic
794 Cluster Therapy (ACT) — pre-clinical proof of principle for local drug delivery and enhanced
795 uptake, Journal of Controlled Release, 224 (2016) 158-164.
796 [77]G. Dimcevski, S. Kotopoulis, T. Bjånes, D. Hoem, J. Schjøtt, B.T. Gjertsen, M. Biermann, A.
797 Molven, H. Sorbye, E. McCormack, M. Postema, O.H. Gilja, A human clinical trial using ultrasound
798 and microbubbles to enhance gemcitabine treatment of inoperable pancreatic cancer, Journal of
799 Controlled Release, 243 (2.172-181 (016
800 [78]T. Li, Y.-N. Wang, T.D. Khokhlova, S. D'Andrea, F. Starr, H. Chen, J.S. McCune, L.J. Risler, A.
801 Mashadi-Hossein, S.R. Hingorani, A. Chang, J.H. Hwang, Pulsed High-Intensity Focused Ultrasound
802 Enhances Delivery of Doxorubicin in a Preclinical Model of Pancreatic Cancer, Cancer research, 75
803 (2015) 3738-3746.
804 [79]S.K. Golombek, J.-N. May, B. Theek, L. Appold, N. Drude, F. Kiessling, T. Lammers, Tumor
805 targeting via EPR: Strategies to enhance patient responses, Advanced drug delivery reviews, 130
806 (2018) 17-38.
807 [80]A. Schroeder, R. Honen, K. Turjeman, A. Gabizon, J. Kost, Y. Barenholz, Ultrasound triggered
808 release of cisplatin from liposomes in murine tumors, Journal of Controlled Release, 137 (2009)
809 63-68.
810 [81]M. Talelli, M. Iman, A.K. Varkouhi, C.J.F. Rijcken, R.M. Schiffelers, T. Etrych, K. Ulbrich, C.F.
811 van Nostrum, T. Lammers, G. Storm, W.E. Hennink, Core-crosslinked polymeric micelles with
812 controlled release of covalently entrapped doxorubicin, Biomaterials, 31 (2010) 7797-7804.
813 [82]S. Murty, T. Gilliland, P. Qiao, T. Tabtieng, E. Higbee, A. Al Zaki, E. Pure, A. Tsourkas,
814 Nanoparticles functionalized with collagenase exhibit improved tumor accumulation in a murine
815 xenograft model, Part Part Syst Charact, 31 (2014) 1307-1312.
816 [83]V.P. Torchilin, Multifunctional, stimuli-sensitive nanoparticulate systems for drug delivery,
817 Nature Reviews Drug Discovery, 13 (2014) 813.
818 [84]Y. Tsvetkova, N. Beztsinna, M. Baues, D. Klein, A. Rix, S.K. Golombek, W.e. Al Rawashdeh, F.
819 Gremse, M. Barz, K. Koynov, S. Banala, W. Lederle, T. Lammers, F. Kiessling, Balancing Passive and
820 Active Targeting to Different Tumor Compartments Using Riboflavin-Functionalized Polymeric
821 Nanocarriers, Nano letters, 17 (2017) 4665-4674.
822 [85]M. Talelli, C.J.F. Rijcken, S. Oliveira, R. van der Meel, P.M.P. van Bergen en Henegouwen, T.
823 Lammers, C.F. van Nostrum, G. Storm, W.E. Hennink, Nanobody — Shell functionalized
824 thermosensitive core-crosslinked polymeric micelles for active drug targeting, Journal of
825 Controlled Release.183-192 (2011) 151 ,
826 [86]T. Lammers, W.E. Hennink, G. Storm, Tumour-targeted nanomedicines: principles and
827 practice, British journal of cancer, 99 (2008) 392.
828 [87]L.M.P. Vermeulen, S.C. De Smedt, K. Remaut, K. Braeckmans, The proton sponge hypothesis:
829 Fable or fact?, European journal of pharmaceutics and biopharmaceutics : official journal of
830 Arbeitsgemeinschaft fur Pharmazeutische Verfahrenstechnik e.V, 129 (2018) 184-190.

[88]S.C. Yang, H.X. Ge, Y. Hu, X.Q. Jiang, C.Z. Yang, Doxorubicin-loaded poly (butylcyanoacrylate) nanoparticles produced by emulsifier-free emulsion polymerization, Journal of applied polymer science, 78 (2000) 517-526.
[89]M. Faria, M. Björnmalm, K.J. Thurecht, S.J. Kent, R.G. Parton, M. Kavallaris, A.P.R. Johnston, J.J. Gooding ,S.R. Corrie, B.J. Boyd, P. Thordarson, A.K. Whittaker, M.M. Stevens, C.A. Prestidge, C.J.H. Porter, W.J. Parak, T.P. Davis, E.J. Crampin, F. Caruso, Minimum information reporting in bio–nano experimental literature, Nature Nanotechnology, 13 (2018) 777-.785
[90]B. Thézé, N. Bernards, A. Beynel, S. Bouet, B. Kuhnast, I. Buvat, B. Tavitian, R. Boisgard, Monitoring therapeutic efficacy of sunitinib using [18F]FDG and [18F]FMISO PET in an immunocompetent model of luminal B (HER2-positive)-type mammary carcinoma, BMC cancer, 15 (2015) 534.
[91]V. Huber, C. Camisaschi, A. Berzi, S. Ferro, L. Lugini, T. Triulzi, A. Tuccitto, E. Tagliabue, C. Castelli, L. Rivoltini, Cancer acidity: An ultimate frontier of tumor immune escape and a novel target of immunomodulation, Seminars in cancer biology, 43 (2017) 74-89.
[92]M. Bellone, A. Calcinotto, P. Filipazzi, A. De Milito, S. Fais, L. Rivoltini, The acidity of the tumor microenvironment is a mechanism of immune escape that can be overcome by proton pump inhibitors, Oncoimmunology, 2 (2013) e22058.
[93]S. Pilon-Thomas, K.N. Kodumudi, A.E. El-Kenawi, S. Russell, A.M. Weber, K. Luddy, M. Damaghi, J.W. Wojtkowiak, J.J. Mule, A. Ibrahim-Hashim, R.J. Gillies, Neutralization of Tumor Acidity Improves Antitumor Responses to Immunotherapy, Cancer research, 76 (2016) 1381-1390.
[94]A. Lardner, The effects of extracellular pH on immune function, Journal of leukocyte biology, 69 (2001) 522-530.
[95]C. Corbet, O. Feron, Tumour acidosis: from the passenger to the driver's seat, Nature reviews. Cancer, 17 (2017) 577-593.
[96]F. Hirschhaeuser, U.G. Sattler, W. Mueller-Klieser, Lactate: a metabolic key player in cancer, Cancer research, 71 (2011) 6921-6925.